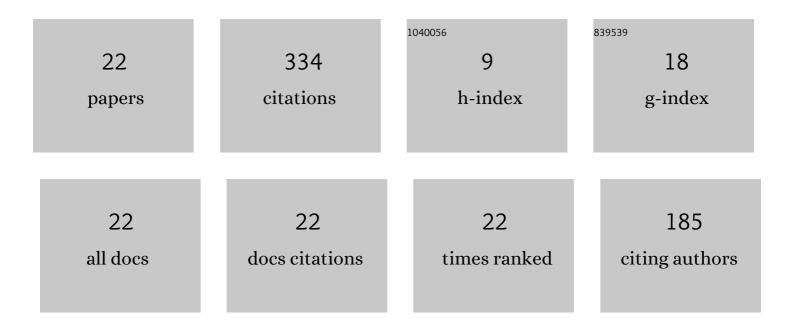


List of Publications by Year in descending order

Source: https://exaly.com/author-pdf/1941986/publications.pdf Version: 2024-02-01



ΙΙΔΝΙ ΧΤΙ

#	Article	IF	CITATIONS
1	Study on the relationship between Fe3O4 fouling and NiFe2O4 oxide layer in the secondary circuit of nuclear steam generator. Surface Science, 2022, 717, 122001.	1.9	4
2	Fouling on the secondary side of nuclear steam generator tube: Experimental and simulated study. Applied Surface Science, 2022, 590, 153143.	6.1	7
3	Microstructural Characterization of the Corrosion Product Deposit in the Flow-Accelerated Region in High-Temperature Water. Crystals, 2022, 12, 749.	2.2	2
4	Dissolution Behaviour of Laves Phase in P92 High Alloy Steel in Alkaline Solutions. Journal of the Electrochemical Society, 2021, 168, 031505.	2.9	3
5	Acoustic emission behaviour during the evolution of a single pit on stainless steels. Corrosion Science, 2021, 183, 109308.	6.6	5
6	DFT studies on the interaction of Fe2+/Fe3O4(1 1 1) and OH-/Fe3O4(1 1 1) during the adsorption process in the steam generators of nuclear power plants. Colloids and Surfaces A: Physicochemical and Engineering Aspects, 2021, 617, 126393.	4.7	11
7	Correlation between the fouling of different crystal calcium carbonate and Fe ₂ O ₃ corrosion on heat exchanger surface. Molecular Simulation, 2021, 47, 748-761.	2.0	4
8	Computational study of Fe3O4 adsorption behaviour on the secondary side of the heat exchange tube in the steam generator. Computational Materials Science, 2021, 195, 110471.	3.0	6
9	Effects of alternating dissolved oxygen and dissolved hydrogen on the corrosion behavior of alloy 52 in high temperature high pressure water. Journal of Nuclear Materials, 2020, 540, 152396.	2.7	3
10	Mechanistic Understanding of the Dissolution Behavior of the Precipitates in 12Cr Martensitic Steel during Potentiodynamic Polarization in Strong Alkaline Solutions. Journal of the Electrochemical Society, 2020, 167, 141501.	2.9	4
11	The SCC initiation behavior of Alloy 600 during the transition of hydrogenated/oxygenated water condition at evaluated temperature. Materials Letters, 2019, 241, 235-238.	2.6	2
12	An electrochemical method for detection and quantification of Laves phase in 12Cr martensitic stainless steel. Corrosion Science, 2018, 135, 215-221.	6.6	13
13	The oxidation behavior of 316L in simulated pressurized water reactor environments with cyclically changing concentrations of dissolved oxygen and hydrogen. Journal of Nuclear Materials, 2018, 511, 417-427.	2.7	9
14	Microstructure and pitting behavior of the dissimilar metal weld of 309L cladding and low alloy steel A533B. Journal of Nuclear Materials, 2018, 508, 1-11.	2.7	24
15	Effects of hydrogen on corrosion of pure Ni in high temperature water. Corrosion Science, 2017, 122, 123-129.	6.6	14
16	The corrosion behavior of Alloy 182 in a cyclic hydrogenated and oxygenated water chemistry in high temperature aqueous environment. Corrosion Science, 2016, 104, 248-259.	6.6	24
17	The corrosion behavior of Alloy 52 weld metal in cyclic hydrogenated and oxygenated water chemistry in high temperature aqueous environment. Journal of Nuclear Materials, 2015, 461, 10-21.	2.7	28
18	The effects of dissolved hydrogen on the corrosion behavior of Alloy 182 in simulated primary water. Corrosion Science, 2015, 97, 115-125.	6.6	44

Jian Xu

#	Article	IF	CITATIONS
19	Acoustic emission response of sensitized 304 stainless steel during intergranular corrosion and stress corrosion cracking. Corrosion Science, 2013, 73, 262-273.	6.6	48
20	Acoustic emission during the electrochemical corrosion of 304 stainless steel in H2SO4 solutions. Corrosion Science, 2011, 53, 448-457.	6.6	30
21	Acoustic emission during pitting corrosion of 304 stainless steel. Corrosion Science, 2011, 53, 1537-1546.	6.6	49
22	The Effects of Chloride Ion Concentration on the Pitting Behavior of 309L Cladding by Using Micro-Electrochemical Measurement and In Situ Optical Observation. Journal of Materials Engineering and Performance, 0, , 1.	2.5	0